Dangerous stellar encounters with an Earth-like planet in the Milky Way galaxy

Behzad Bojnordi Arbab,⋆ Sohrab Rahvar,†
Department of Physics, Sharif University of Technology, P.O. Box 11155-9161, Tehran, Iran

ABSTRACT
In this work, we study the orbital resilience of an Earth-like habitable planet in the gravitational collision with the stars of the Milky Way. Our criterion is that the planet during this collision does not move outside the habitable zone. In this simulation, we use the gravitational interaction of the three-body objects of the parent star, the Earth-like planet, and the encountering star. Our simulation shows that the rate of dangerous encounters (moving away from the habitable zone) is $\Gamma = 3.73 \times 10^{-6}$/Gyr for the solar neighborhood and $\Gamma = 6.12 \times 10^{-4}$/Gyr for the bulge environment. Comparing this result with the time-scale of life on Earth ($\sim$ 4Gyr), the probability of life extinction due to the gravitational interaction of the planetary system with the encountering stars is negligible.

Key words: stars: kinematics and dynamics – planets and satellites: dynamical evolution and stability – Galaxy: general

1 INTRODUCTION

The discovery of other planets harboring life is one of the most ambitious projects in astronomy, and Earth-like planets in habitable zones around stars are the main expected environment to find life. Habitable zone (HZ) is the region around stars where a rocky planet with its atmosphere can support liquid water. For a planet located in this region, life can potentially emerge, sustain and evolve (Huang 1959, 1960; Kasting et al. 1993; Kopparapu et al. 2013). However, there might be catastrophic events that threaten the existence of life on the planets. We can categorize the catastrophic events into terrestrial and extra-terrestrial classes.

Terrestrial catastrophic events: Various events originated from the planet can cause mass extinctions. For instance, rapid volcanic activities and eruptions can cause catastrophic climate changes (Wignall 2001). Several mass-extinctions have been characterized to be coinciding with mass-volcanism events (Alvarez 2003), although some investigations suggest astronomical events to be in charge. For example, Pandey & Negi (1987) indicates that volcanic activity periodicity coincides with the period of sun crossing the Galactic disk. Abbott & Isley (2002) claim a correlation between volcanic activity and the asteroid impact rate history of Earth and Moon. Other terrestrial catastrophes such as drop and rise in sea level, oxygen deficiency of oceanic

waters, continental drift, mountain building, and submarine methane release are candidates for historical and future possible mass extinctions (Bailer-Jones 2009).

Extraterrestrial catastrophic events: Another origin for life-threatening catastrophes comes from the astronomical interactions. Our main focus in this paper is an extraterrestrial event, therefor we enlist the most studied catastrophes of this kind.

Impact of comets or asteroids: A major-impact of an asteroid or comet can cause life-threatening catastrophes in a wide range of danger, from threatening many species to wiping out life from the face of Earth. The typical interval of such impacts ranges from 10^5 years (for lower catastrophe limits) to 10^8 years (for imminent global catastrophes) (Chapman & Morrison 1994). An increase in cometary and asteroidal impact rate can be hazardous to terrestrial life. Almost all long-period comets come from the Oort cloud (Oort 1950). Due to perturbations, comets may inject into the inner solar system region. The outer Oort cloud radius is comparable to the distance of nearby stars and as a result, the gravitational force of a stellar encounter can induce a shower of comets into the inner planetary system, increasing major-impact rates (Hills 1981; Matese & Lissauer 2002; Wickramasinghe & Napier 2008). Using the nearby stars astrometric data obtained from catalogs such as Hipparcos and Tycho (ESA 1997) and Gaia (Gaia Collaboration et al. 2018), the occurrence of such encounters can be predicted or the past ones are discovered. Bobylev (2017) studied the possible past and future stellar encounters from

⋆ E-mail: bojnoordi_b_@physics.sharif.edu
† E-mail: rahvar@sharif.edu

nearby stars that can produce the perturbations in the Oort cloud. Bailer-Jones (2017) utilized data from the first Gaia data release (GDR1) and other projects, and integrating the stellar motions through Galactic potential, identified close stellar encounters comparable to the Oort cloud. More recently, Bailer-Jones et al. (2018) implemented almost the same method for the second Gaia data release (GDR2).

Periodically passing of solar system into the galactic plane can increase the stellar density, resulting in an increase in stellar encounters (Heisler & Tremaine 1986; Matese et al. 1995). As a result of the gigantic size of the Oort cloud and the weak binding of the cloud to the solar gravitation, the tidal force of the Galaxy and a dark matter disk can also induce enough perturbation to alter the rate of comets falling in the inner regions of solar system (Rampino 2015).

Giant molecular clouds (GMCs):A giant molecular cloud (GMC) encounter is infrequent but can impose catastrophic effects on the planetary system, such as disturbing the Oort cloud and therefore increasing the rate of cometary impacts (Mazeeva 2004; Jakubík & Neslušan 2008). The passing of a planetary system through a GMC can also affect the climate by increasing the influx of cometary dust (Hoyle & Lyttleton 1939; Shaviv 2003). Moreover, the increased interplanetary medium density during the encounter can terminate the solar wind and affect the planetary climate, or even produce an ice age (Begelman & Rees 1976).

Supernova events: Radiation from the initial blast and remnant of a nearby supernova event produces enough radiation energy and cosmic rays to disrupt planetary climate and Ozone layer, and even change the characteristics of protoplanetary systems. During a supernova, the nearby planetary systems experience an increase in cosmic-ray flux, e.g. 2-3 order of magnitude for a supernova in 12-15pc distance (Tanaka 2006). It is suggested that a rise in cosmic-ray flux increases cloud-nucleation and therefore, can increase the cloud coverage on the planet (Kirkby 2007). Also, a supernova event in the neighborhood can result in the destruction of Ozone layer, due to production of NO, which reacts with O_3 molecules and deplete the Ozone layer (Ruderman 1974; Gehrels et al. 2003). Such events can happen 4 times every billion year on average for 10pc distant supernovae (Rahvar 2017). A supernova in 0.5pc distance can truncate the outer edge of a protoplanetary disk and tilt the disk (Zwart et al. 2018). As a result, the effects of a nearby supernova can be threatening for both life-harboring planets and future habitable planetary systems.

Close stellar encounters can gravitationally affect planetary systems and cause habitability catastrophes, however, such an encounter is very rare compared to the other discussed catastrophes. Such events can directly change the orbital parameters of the planets during the encounter, or disrupt the interplanetary resonances or the protoplanetary disks. In this work, we investigate a specific catastrophe event, where a stellar encounter results in the exit of an Earth-like planet from its habitable zone. Some of the first attempts for calculating the effects of close stellar encounters on planetary orbital parameters have been studied in terms of initial parameters of the planetary orbit and the initial encountering stellar parameters (Lyttleton & Yabushita 1965). In the early numerical investigations, the encounters revealed that the energy and the angular momentum trans-

fer between the parent star, the planet and the encountering star (Clarke & Pringle 1991; Hall et al. 1996; Ostriker 1994).

In the early formation-period of a planetary system, stellar encounters can be critical in the properties of later protoplanetary disks and the planetary system. Kobayashi & Ida (2001) investigated the changes in eccentricity, inclination, and longitude alignments of the protoplanets in inner and outer regions of protoplanetary disks, caused by an encounter event. Stellar encounters can also shrink the size of protoplanetary disks. Vincke et al. (2015) investigated the truncation of the disks in different cluster populations, showing that for birth clusters like Orion Nebula Cluster, stellar encounters play an important role in shaping the protoplanetary disks. Stellar encounters in young clusters can even strip stars from debris disks (Lestrade et al. 2011), change eccentricity, capture or send the planets out of the planetary system (Li & Adams 2015; Malmberg et al. 2011; Jiménez-Torres et al. 2011). However, the consequences of stellar encounters can be altered or canceled through dynamical processes of later planetary formation stages. Marzari & Picogna (2013) and Picogna & Marzari (2014) showed that the circumstellar disk can erase the stellar encounter effects on protoplanets eccentricities in ≈ 10 kyr during the stay in the birth cluster, but the semi-major axes do not revert to the initial sizes. Portegies Zwart & Jílková (2015) distinguished the circumstellar regions in open clusters based on gravitational effects from external and internal planetary system influences by defining Parking Zone and Frozen zone. These zones specify the size of the circumstellar orbital space mainly uninfluenced by stellar encounters. Incidents of stellar encounters in dense clusters changes the population of planets and plays an important role in planetary formation procedures (Jiménez-Torres et al. 2011; Fragner & Nelson 2009; Craig & Krumholz 2013; Malmberg et al. 2011).

In this work, we specifically focus on the persistence of the planetary orbit in the habitable zone due to the encounters, especially for the case of Earth-like planets. We will investigate the time-scale of planets being stable in their habitable zone and compare it with the age of life on Earth. This time-scale depends on the environment by the mean of the stellar populations and density of stars. We compare our results in the disk with the Galactic bulge. Note that we use a simplified close stellar encounter catastrophe; the changes in other planetary orbits and the inter-planetary gravitational effects are not studied.

This paper is organized as follows. In section (2), we express the methods used for simulating the close stellar encounters, defining the dangerous impact-parameter, dangerous cross-section and dangerous impact rate. In section (3), we study the correlations between the dangerous impact parameter, the initial parameters of the encountering star, and the habitable zone width, and finally, calculate the dangerous encounter rates for the solar system neighborhood and the Milky Way bulge. The conclusion is given in section (4)

2   METHODS AND IMPLEMENTATION

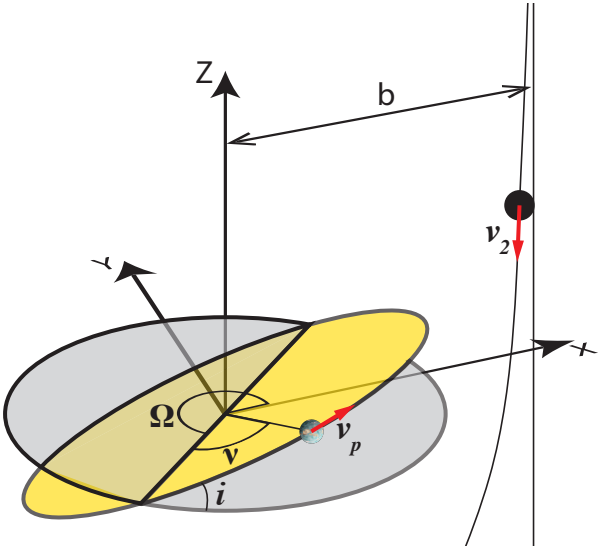In this section, we begin by introducing the close stellar encounter and associated parameters.Also, we discuss the

Figure 1. The orbital parameters of encounters is as follows: b is the impact parameter of the secondary star with respect to the parent star, v_2 is the initial velocity of the secondary star, v_p is the initial orbital velocity of the planet, Ω is the longitude of the ascending node, i is the inclination of the planetary orbit with respect to the (x-y) plane and ν is the initial anomaly of the planets measured counterclockwise from the ascending node.

rate of encounters that can deviate the planet's orbit from the habitable zone.

2.1 Methods

For simplicity, we assume a gravitational system consisting of three bodies: (i) the parent star, (ii) the orbiting planet around the parent star, and (iii) the encountering star. We simplify the physics of encountering by assuming that the target star has one planet, where together with the encountering star, makes a three-body gravitational interaction. For the encountering stars, we use the kinematic and the stellar population of stars in Galaxy while we adapt the target star as a solar-type star and the planet as an Earth-type planet (García-Sánchez et al. 2001). Here for simplicity, we ignore the encountering binary and multiple stars.

For the numerical calculation, we use the gravitational integrations for the stellar encounter by the REBOUND code[1] (Rein & Liu 2011) and the IAS15 algorithm (Rein & Spiegel 2014), which is a 15th-order gravitational dynamics integrator and optimized for integrating close-encounter schemes. The encountering parameters in our study are (i) the velocity and mass of the encountering star (V_2 and M_2), (ii) the impact parameter of the encountering star with respect to the primary star (b), (iii) two angular parameters indicating the orientation of the planetary orbital plane with respect to the encountering star (i.e., Ω and i in Figure 1) and (iv) the initial anomaly of the planet (i.e., ν in Figure 1). We also have a parameter indicating the width of the habitable zone (W_{hz}). Here, we adapt the mass of the parent star to be one solar mass and the mass of the planet to be one earth mass.
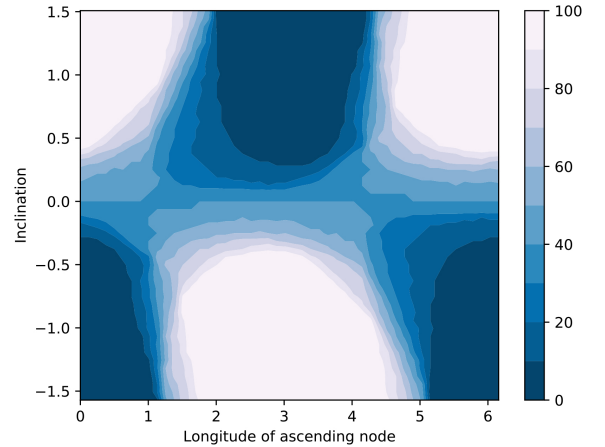
Figure 2. Probability function of the planetary orbit remain in the habitable zone. Here we adapt $M_2 = 1 M_\odot$, $V_2 = V_p$ and $b = 4 a_p$ and the the primary system is identical to the sun-earth parameters, and Kasting et al. (1993) conservative instantaneous HZ is used.

We place the origin of the Cartesian coordinate system on the position of the parent star. The secondary star is initially at the position of $(x, y, z) = (b, 0, 50 AU)$, along the z axis in this coordinate. Two angular parameters are required to specify the initial alignment of planet orbit in this coordinate system; the inclination angle of "i" from the xy plane and the longitude of the ascending node (Ω) of the planetary orbit which is measured from the x-axis. Also, we measure the anomaly of the planet (i.e., ν) from the ascending node, counterclockwise on the planet's orbital plane.

In our simulation, we scan all the mentioned parameter space with the following range of $\Omega \in [0, 2\pi]$, $\nu \in [0, 2\pi]$, $i \in [-\pi/2, \pi/2]$, $b \in [0.1, 100] a_p$ where a_p is the planet orbital radius. All the parameters are chosen with uniform distribution functions. The kinematic parameters such as V_2 and the mass of the secondary star, M_2 have their own distribution functions and will be discussed in the next section. For each run of the simulation, the initial parameters are selected from the mentioned 6-dimension space and finish the calculation of the dynamics when the encountering star reaches the distance of $z = -50$ AU far from the primary star. After the encounter, we calculate the orbital parameters of the planet. An event is a "dangerous encounter" if perturbations from the encountering star push the planet out of the habitable zone via the inner or outer boundaries of HZ, or is a "safe encounter" if it stays in the HZ after the encounter. In each encounter, the total numerical relative energy error is less than $\Delta E/E < 10^{-14}$, and the total numerical relative angular momentum error is less than $\Delta L/L < 10^{-15}$.

Figure (2) demonstrates an example from our simulation where we fix three parameters of $M_2 = 1 M_\odot$, $V_2 = V_p$ and $b = 4 a_p$ and the the primary system is adapted to be identical to the sun-earth parameters. Here V_p is the orbital velocity of the planet around the parent star. In this figure, we identify stellar encounters in terms of Ω versus i integrated over all the values of anomalies, showing the Probability function for the planet remaining in the habitable zone of the parent star (P_{HZ}).
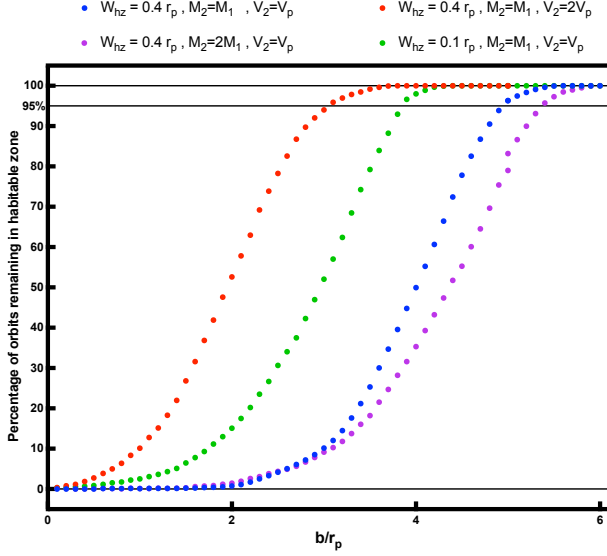
Figure 3. Percentage of orbits remaining in the habitable zone for different initial conditions.

In what follows, we classify the parameters of this problem into two groups as (M_2, V_2, b, W_{hz}) and the second group identifying the angular orientation of the planet as $(i, \Omega$ and $\nu)$. We will integrate over the parameters in the second group to provide the probability function of a planet remain in the HZ (i.e., P_{HZ}) in terms of the first group of parameters. Figure (3) represents another example from our simulation where we calculate P_{HZ} as a function of impact parameter for various sets of the mass and the velocity of encountering stars and the width of the habitable zone. From Figure (3), we define the "dangerous impact parameter" (b_d) as the largest impact parameter where P_{HZ} is less than 95%. In Figure (3), corresponding the largest impact parameter is identified.

We study the relationship between the dangerous impact parameter (b_d) and physical parameters such as the width of the habitable zone boundary (W_{hz}), velocity (V_2) and mass (M_2) of the encountering star, integrating over the rest of the parameter space. Here we simulate 8000 encounters for each set of physical parameters with scanning uniformly over i, Ω, and ν. From the dangerous impact parameter, we can calculate the associated cross-section and, finally, the rate of the dangerous encounters.

2.2 Encounter rate calculation

In order to calculate the rate of dangerous encounters, we calculate the cross-section for dangerous impact parameter as follows

$$\sigma_d = \pi b_d^2 \ , \tag{1}$$

We note that the cross-section is a function of velocity and the mass of the secondary star and the width of the habitable zone. From the definition of the cross-section, the dangerous encounter rate is given by (Hut & Tremaine 1985; García-Sánchez et al. 2001; Li & Adams 2015)

$$\Gamma_d = n_\star \langle \sigma_d \rangle_{(V)} \sqrt{V_\odot^2 + V_\star^2} \ , \tag{2}$$

where $V_\odot$ is the peculiar velocity of the sun in local standard of rest in the solar neighborhood (Bobylev & Bajkova 2014), $V_\star$ is the velocity dispersion of stars, $n_\star$ is the number density of the stars in the environment, and $\langle \sigma_d \rangle_{(V)}$ is the averaged dangerous cross-section over a Maxwell Boltzmann density function of the stellar velocities in the environment $f_{(V)}$. The Maxwell Boltzmann probability density function is:

$$f_{(V)} = \sqrt{\frac{2}{\pi}} \frac{V^2 e^{-\frac{V^2}{2\alpha^2}}}{\alpha^3}, \tag{3}$$

where α is the scale parameter, which has the following relationship with the velocity dispersion:

$$V_\star = \sqrt{\frac{\alpha^2(3\pi - 8)}{\pi}}, \tag{4}$$

therefore, the probability density function with regard to the velocity dispersion is:

$$f_{(V)} = \frac{\sqrt{2(3\pi - 8)^3}}{\pi^2 V_\star^3} V^2 e^{-\frac{(3\pi-8)V^2}{2\pi V_\star^2}} \ . \tag{5}$$

3 RESULTS

In this section, we present the underlying aims of the research. We study the relationship between the dangerous impact parameter with the physical parameters (i.e., the velocity and the mass) of the encountering star. Then, the relation of the dangerous impact parameter with the width of the habitable zone for various ranges is studied. We also study the effect of the inclination angle of the orbital plane of the planet on dangerous encounters. This section concludes by presenting the results for dangerous cross-section and dangerous impact rates for various types of encountering stars. We also present the total dangerous impact rate and the probability of such impacts in the 4-billion years period. We use Kasting et al. (1993) conservative definition of instantaneous HZ (and we call it Kasting HZ) throughout this paper, unless indicated otherwise.

3.1 The relation between the dangerous impact parameter and the velocity of the secondary star

In order to investigate the relationship between the dangerous impact parameter and the initial velocity of the encountering star, we simulated systems with a broad range of velocities compare to the dispersion velocity of stars. In Figure (4), we plot the dangerous impact parameter normalized to the orbital radius of the planet, as a function of the relative velocity of encountering star with respect to the velocity of the planet. Here we have different scaling relation of the power of ~ -1 for the small and power of ~ -0.5 for the large velocities of the encountering stars.

We can interpret Figure (4) from the rough analysis of the gravitational impact. Let us use the generic relation between the minimum encounter distance (i.e., r_{min}) and impact parameter (i.e., b) (Hills 1984) from the three body
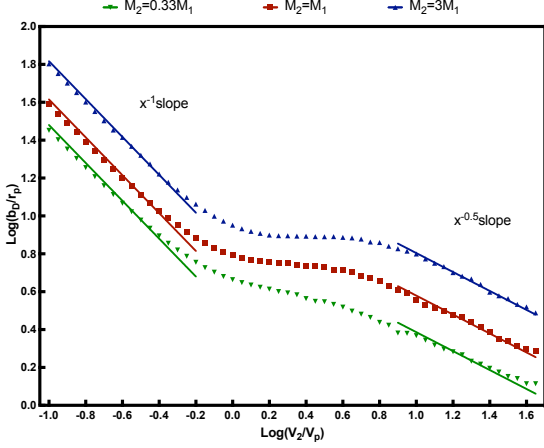
Figure 4. The dangerous impact parameter normalized planetary orbital radius, as a function of the relative velocity of the encountering star with respect to the velocity of the planet, both in logarithm scales. The three datasets are for different secondary star masses; $M_2 = 0.3M_1$, $M_2 = M_1$, $M_2 = 3M_1$, and Kasting HZ is used.

problem as follows

$$r_{min} = a_c \left(\left[1 + \left(\frac{b}{a_c} \right)^2 \right]^{1/2} - 1 \right) , \qquad (6)$$

where

$$a_c = \frac{G(M_1 + M_2)}{V_2^2}, \qquad (7)$$

and a_c is the accretion radius, parameterizing the gravitational focusing.

High velocity regime: In the case of a distant encounter and high relative velocities ($V_2 \gg V_P$) the gravitational impulse (ΔI) at the given distance from the star is proportional to (Martínez-Barbosa et al. 2017)

$$\Delta I \propto \frac{M_2}{V_2 r_{min}^2}. \qquad (8)$$

For the high velocities of encountering star, from the combination of equation (6) and equation (7), we can conclude that r_{min} is almost equal to the impact parameter, b. As a result from equation (8) for a given impulse, to push the planet out of the habitable zone,

$$b_d \propto V_2^{-0.5} . \qquad (9)$$

Low velocity regime: For the low relative velocities of the two stars (i.e.,$V_2 < V_p$), from equation (6), $r_{min} = \frac{1}{2} \frac{b^2}{a_c}$ where substituting the definition of a_c from equation (7) results in

$$b_d \approx \frac{[2 r_{min} G(M_1 + M_2)]^{1/2}}{V_2}. \qquad (10)$$

So the dangerous impact parameters related to the initial velocity of the secondary star as $b_d \propto V_2^{-1}$.

The dangerous impact parameter as a function of the low and high velocity regimes of the secondary star is consistent with Figure (4).
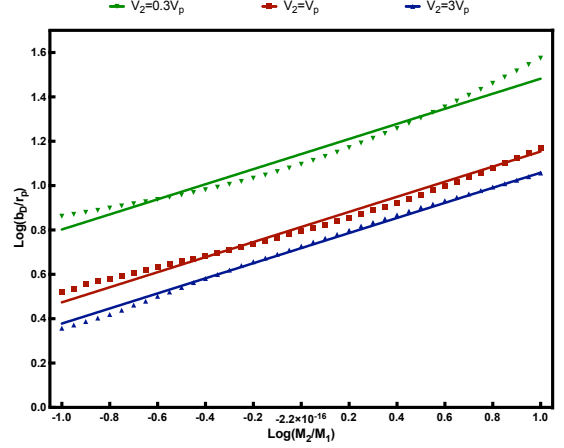
Figure 5. Log-Log plot of the dangerous impact parameter as a function of the mass of the secondary star, relative to the primary star for three different velocities. plotted for three different velocities: $V_2 = 0.3V_p$, $V_2 = V_p$ and $V_2 = 3V_p$. Kasting HZ boundaries are used.

3.2 Relation between the dangerous impact parameter and the mass of the secondary star

The relative mass of the secondary star to the primary star (i.e.,M_2/M_1) plays a significant role in the size of the dangerous impact parameter. We performed simulations for the relative mass in the range of $0.1 < M_2/M_1 < 10$.The results of our simulation are represented in Figure (5) for the impact parameter in terms of the relative masses for three different velocities of the secondary star. By increasing the mass of the secondary star, the tidal forces on the star-planet system increases, and the dangerous impact parameter occurs in the larger distances.

Fitting the numerical results with a power-law function results in

$$\frac{b_d}{a_p} \propto \left(\frac{M_2}{M_1} \right)^{0.34} . \qquad (11)$$

This equation is almost similar to the Hill radius, $r_H \propto (M_2/M_1)^{1/3}$, which represents the unstable sphere around the primary star in the binary system. However, we note that in the Hill radius $M_2 \ll M_1$, unlike to the system in our concern. Also, b_d is the impact parameter of the encounter, rather than the minimum distance of the stars.

3.3 Relation between the dangerous impact parameter and width of the habitable zone

In the previous sections, we have used a fixed habitable zone boundary. The HZ around the sun depends on the criteria on the planetary climate models. Hart (1979) calculated the inner and outer boundary to be 0.95 au and 1.01 au, respectively. Kasting et al. (1993) identified conservative instantaneous HZ to be between 0.95 au to 1.37 au, conservative continuous HZ to be 0.95 au to 1.15 au, and optimistic instantaneous habitable zone to be in the 0.84 au to 1.67 au, respectively. Kopparapu et al. (2013) also estimated the HZ boundaries to be 0.99 au and 1.70 au. In this section, we let the habitable width to be a free parameter and study the
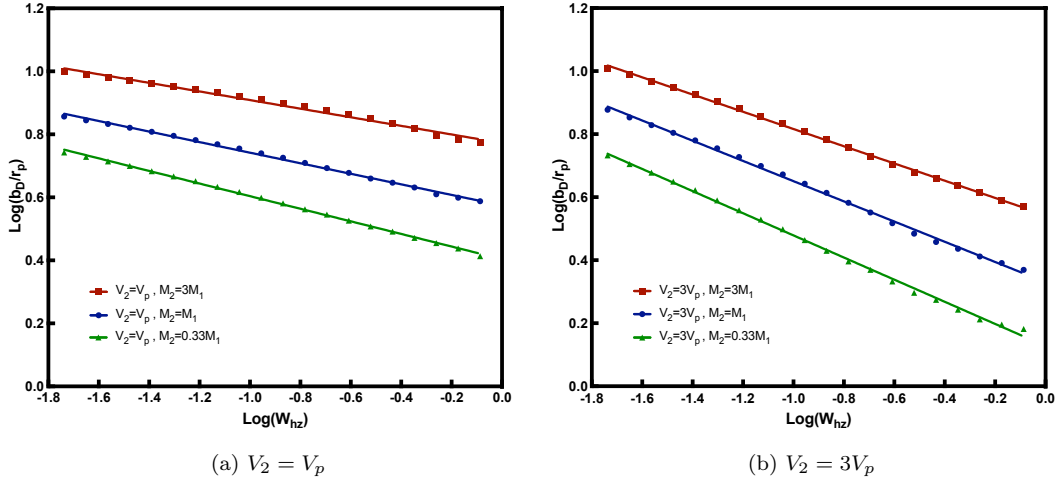
Figure 6. The dangerous impact parameter in logarithmic scale as a function of W_{hz} in logarithmic scale with three different M_2 values. The two figures differ in the velocity of the encountering star (V_2). As shown, the relationship between dangerous impact parameter and W_{hz} is a power law (linear in Log-Log plot), with different powers, depending on V_2 and M_2. We interpret the dependence of dangerous impact parameter to M_2 in equation (11).

dangerous impact parameter in terms of the width of the habitable zone.

In the simulations, we adopt the position of the planet to be in the median radius of the habitable zone. The result of our simulation is shown in Figure (6) for three different mass-ratios and two different initial velocities of the secondary star. The scaling relation between the dangerous impact parameter and the width of the habitable zone is a power-law function as $b_d \propto W_{hz}^\alpha$ where $\alpha < 0$ and it is a function of the stellar mass ratio (M_2/M_1) and the initial velocity of the secondary star (V_2). We note that W_{hz} depends on the stellar type and a model we are adapting for the habitable zone. In our study, we take a solar-type parent star. Our results show that the rate of dangerous encounters has a small dependence on the definition of the habitable zone model.

3.4 The most dangerous orbital inclinations for the encounters

Different inclinations of the planet orbit with respect to the orbital plane of the secondary star changes the ratio of dangerous encounters. In order to study the probability function for the dangerous encounters, we simulated planets with a fixed initial inclination angle and an impact parameter and change the initial anomaly and longitude of ascending node. We integrate over the nuisance parameters (i.e.,ν and Ω) and calculate the ratio of events where the planet remains in the habitable zone for each set of inclination and impact parameter, as shown in Figure (7). For a given impact parameter, a dangerous impact depends on the inclination angle where for large impact parameters, larger inclination (almost parallel to the planetary orbit) are more dangerous and for the small impact parameter the smaller inclinations (almost perpendicular to the planetary orbit) are the dangerous encounters. Averaging over the impact parameters, the dangerous encounter is not sensitive to the inclination angle.
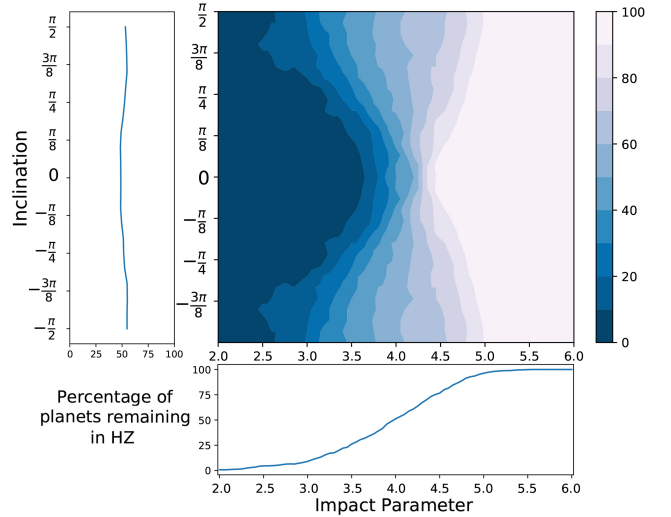

Figure 7. The ratio of events that the planet remains in the habitable zone, as a function of the inclination angle of the planetary orbital plane, and the impact parameter. For impact parameters in the range of $b/a_p < 2$, a hundred percent of events are dangerous encounters, and for $b/a_p > 6$, none of the encounters are dangerous. Here, we have integrated over the initial anomalies and longitude of ascending node of the planetary orbit. The HZ boundaries used are 0.8-1.2 AU.

3.5 Dangerous encounter rate in the solar neighborhood and the Bulge of Milky Way galaxy

From evidence found in old hydrothermal vents, life on earth has been existed for about 4 billion years (Dodd et al. 2017). For an Earth-like planet in order to maintain life like the present Earth, we assume that the planet should be safe for at least 4 billion years. Therefore, our rough estimation of the rate of dangerous encounters should be $\Gamma < 1/4 \text{Gyr}^{-1}$.

We use data of the populations of stars in the solar neighborhood from Rickman et al. (2004), Allen (1973)

Table 1. Populations of stars in the solar neighborhood, with velocity dispersion (in km/s), peculiar velocity of sun (in km/s), mass (in solar mass), and stellar number density (in $10^{-3} pc^{-3}$). Stellar types include MK types for main-sequence stars, white dwarves (WD), and giants. (The data is adapted from Table 8 of García-Sánchez et al. (2001))

Stellar type	$V_\star$ (km/s)	$V_\odot$ (km/s)	$M(M_\odot)$	$n_\star/pc^3 \times 10^{-3}$
B0	14.7	18.6	18	0.06
A0	19.7	17.1	3.2	0.27
A5	23.7	13.7	2.1	0.44
F0	29.1	17.1	1.7	1.42
F5	36.2	17.1	1.3	0.64
G0	37.4	26.4	1.1	1.52
G5	39.2	23.9	0.93	2.34
K0	34.1	19.8	0.78	2.68
K5	43.4	25.0	0.69	5.26
M0	42.7	17.3	0.47	8.72
M5	41.8	23.3	0.21	41.55
WD	63.4	38.3	0.9	3.00
Giants	41.0	21.0	4	0.4

Table 2. The dangerous encounter cross-sections (in the unit of AU^2 and dangerous encounter rate (in the unit of Gyr^{-1}) for the stars listed in Table 1. We also provide the overall rate of dangerous encounter to be 3.72×10^{-6} encounter per Gyr.

Stellar type	$\langle\sigma_d\rangle(AU^2)$	$\Gamma_d/10^{-8}(Gyr^{-1})$
B0	1053	3.59
A0	220	3.71
A5	162	4.67
F0	137	15.7
F5	113	6.94
G0	99.3	16.6
G5	87.1	22.4
K0	80.2	20.3
K5	68.8	43.4
M0	53.1	51.2
M5	28.6	136
WD	71.7	38.2
Giants	231	10.2
Total		372.9

and García-Sánchez et al. (2001) to calculate dangerous encounter rates for each stellar population as shown in Table 1. Using equation (2), we calculate in Table 2 the cross-sections and rates of the dangerous encounters for each population listed in Table 1. The overall dangerous encounter rate is $3.73 \times 10^{-6} Gyr^{-1}$, where for a period of four billion years, the encounter probability is 1.49×10^{-5}. We would expect to have at least one dangerous encounter out of 10^5 earth-like planets.

We repeat the same analysis for dangerous encounter rates in the inner Galactic bulge. Wegg & Gerhard (2013) used the Red Clump Giants (RCGs) from the VVV survey (Saito et al. 2011) and calculated the 3-dimensional density distribution of bulge within the volume of (± 2.2 k$pc \times \pm 1.4$ k$pc \times \pm 1.1$ kpc) surrounding the Galactic center. On the other hand, Portail et al. (2015) created a dynamical model using Wegg & Gerhard (2013) RCGs density measurements and velocity distribution data from Bulge Radial
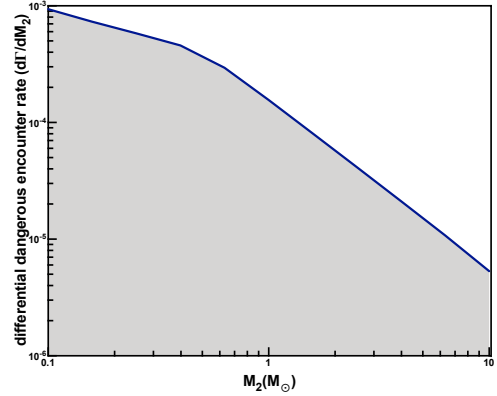
Figure 8. The differential dangerous encounter rates plotted as a function of the secondary star mass in the inner region of Galactic Bulge. The integration of the differential dangerous encounter rate over the secondary star mass (i.e.,the gray area) portraits the total dangerous encounter rate for an Earth-like planet in the region.

Velocity Assay (BRAVA) spectroscopic survey (Rich et al. 2006; Howard et al. 2008; Kunder et al. 2012) and evaluated the stellar mass of the inner Galactic bulge region to be $1.25 - 1.6 \times 10^{10} M_\odot$. From the volume of the bulge and the stellar mass, we estimate the mean stellar-mass density to be ≈ 0.5 $M_\odot/pc^3$.

For simplicity, we assume the Kroupa (2001) initial mass function for the bulge stars, for the mass range of $0.1 M_\odot$ to $10 M_\odot$. The differential dangerous encounter rate is:

$$\frac{d\Gamma}{dM} = \xi(M)\langle\sigma_d\rangle_{(V)} V_\star^{bulge} , \qquad (12)$$

where $\xi(M)$ is the mass function of the bulge which is normalized to the stellar-mass density in the bulge with $\int \xi(M)M dM = \rho_\star$, $\langle\sigma_d\rangle_{(V)}$ is the dangerous cross-section, averaged over velocity and $V_\star^{bulge}$=113km/s is the velocity dispersion of stars in the inner Galactic bulge (Portail et al. 2015). We note that $\langle\sigma_d\rangle_{(V)}$ also depends on the mass of encountering stars.

The results of differential dangerous encounter rate from equation (12) is shown in Figure (8) . By integrating $d\Gamma/dM$ over stellar mass-function, the total dangerous encounter rate is $\Gamma_{total} \approx 6.12 \times 10^{-4} Gyr^{-1}$. This result shows that the catastrophe rate in the Galactic bulge region is about 160 times more than that of in the Solar neighborhood. Interpreting in life-evolution time, out of ≈ 400 Earth-like planets in the inner Galactic bulge region, we expect one planet to face a dangerous encounter in the hypothesized 4-billion-year period required for the evolution of advanced life.

4 CONCLUSIONS

In this work, we studied the close stellar encounters that can disrupt the orbit of habitable planets and deprive the planets of habitability conditions. We took the parent star with the planet as a binary system while the encountering star plays the role of the third gravitating object. Using the numerical calculation for the gravitational interaction, we also considered the gravitational effect of the planet on the parent star and encountering star. In this study, we had six

dimension parameter space for describing this encounter and studied the most dangerous areas of this parameter space.

The parameter space in our study had two (i) geometrical and (ii) dynamical parts. In the geometric part, we have shown that there is a correlation between the inclination angle (i.e.,i) and orbital ascending node (i.e Ω) and encountering impact parameter (i.e.,b) of the planets for the dangerous encounters. For the dynamical parameter space, we had the velocity and the mass of the encountering star and width of the habitable zone. We adapt the parent star and the planet similar to the Sun-Earth system. We defined a dangerous impact parameter where at least 5% of encounters displace the planet from its habitable zone. Our analysis showed a power-law relationship of the dangerous impact-parameter with relative stellar masses of the encountering star and the parent star ($b_d \propto (M_2/M_1)^{0.34}$).

We also studied the effect of velocity of the encountering star. Our simulations showed the high-speed encounters ($V_2 \gg V_p$) have smaller dangerous impact parameters (comparable to the asteroid belt orbital radii), and the impact parameter decreases as $b_d \propto V_2^{-0.5}$. For most of encounters with the speed of the encountering star comparable to the speed of the Earth around the sun (i.e $V_2 \sim V_p$), the dangerous impact parameter is of the order of the orbital radius of Jupiter and Saturn. Also, the dangerous encounters with low-speed encountering stars ($V_2 \ll V_p$) require impact parameters as larger as Uranus orbital radius and the impact parameter decreases with the same rate as the velocity increases ($b_d \propto V_2^{-1}$).

Studying the dependency of dangerous impact parameter with habitable zone width (W_{hz}), a power-law relationship is observed, while the power depends on the velocity of the secondary star (V_2), and the stellar mass-ratio (M_2/M_1). This is an important relationship, affecting the calculations for other models for circumstellar habitable zone (we used Kasting HZ).

Our final results showed that the probability of a dangerous encounter for a Earth-like planet orbiting around a Sun-like star is $\sim 3.73 \times 10^{-6}$/Gyr. The result means that for every 10^5 habitable earth-like planets, only one planet encounters the catastrophe (by means that encountering star displace earth from the habitable zone) in a 4-billion-year period, required for the formation of Earth-like present-day life. We also analyzed the inner Galactic bulge region surrounding the Milky way center for the catastrophe event rates. Utilizing the number density, mass-function and velocity-dispersion of stars in the inner Galactic bulge, we estimated the dangerous encounter rate to be $\Gamma_{total} \approx 6.12 \times 10^{-4} Gyr^{-1}$. In other words, in ≈ 400 stars in the region, one experiences the dangerous stellar encounter in the 4-billion-year period, therefor, the catastrophe rate is roughly 160 times higher in the Galactic Bulge compare to that in the disk. Concluding this work, for an Earth-like type planet orbiting around a solar-type star, the probability of exiting planet from the habitable zone due to stellar encounter with the other stars is negligible.

REFERENCES

Abbott D. H., Isley A. E., 2002, Earth Planet. Sci. Lett., 205, 53
Allen C. W., 1973, Astrophysical quantities, 3rd edn. Atholone Press
Alvarez W., 2003, Astrobiology, 3, 153
Bailer-Jones C. A., 2009, Int. J. Astrobiol., 8, 213
Bailer-Jones C. A., 2017, Proc. Int. Astron. Union, 12, 144
Bailer-Jones C. A., Rybizki J., Andrae R., Fouesneau M., 2018, Astron. Astrophys., 616
Begelman M. C., Rees M. J., 1976, Nature, 261, 298
Bobylev V., 2017, arXiv.org, 61, 883
Bobylev V. V., Bajkova A. T., 2014, Mon. Not. R. Astron. Soc., 441, 142
Chapman C. R., Morrison D., 1994, Nature, 367, 33
Clarke C. J., Pringle J. E., 1991, Mon. Not. R. Astron. Soc., 249, 584
Craig J., Krumholz M. R., 2013, Astrophys. J., 769, 150
Dodd M. S., Papineau D., Grenne T., Slack J. F., Rittner M., Pirajno F., Jonathan O., Little C. T. S., 2017, Nature, 543, 60
ESA 1997, in Eur. Sp. Agency, (Special Publ. ESA SP).
Fragner M. M., Nelson R. P., 2009, Astron. Astrophys., 505, 873
Gaia Collaboration et al., 2018, Astron. Astrophys., 616, A1
García-Sánchez J., Weissman P. R., Preston R. A., Jones D. L., Lestrade J.-F. F., Latham D. W., Stefanik R. P., Paredes J. M., 2001, Astron. Astrophys., 379, 634
Gehrels N., Laird C. M., Jackman C. H., Cannizzo J. K., Mattson B. J., Chen W., 2003, Astrophys. J., 585, 1169
Hall S. M., Clarke C. J., Pringle J. E., 1996, Mon. Not. R. Astron. Soc., 278, 303
Hart M. H., 1979, Icarus, 37, 351
Heisler J., Tremaine S., 1986, Icarus, 65, 13
Hills J. G., 1981, Astrophys. J., 86, 1730
Hills J. G., 1984, Astron. J., 89, 1559
Howard C. D., Rich R. M., Reitzel D. B., Koch A., De Propris R., Zhao H., 2008, Astrophys. J., 688, 1060
Hoyle F., Lyttleton R. A., 1939, Math. Proc. Cambridge Philos. Soc., 35, 405
Huang S.-S., 1959, Publ. Astron. Soc. Pacific, 71, 421
Huang S.-S., 1960, Publ. Astron. Soc. Pacific, 72, 489
Hut P., Tremaine S., 1985, 90, 1548
Jakubík M., Neslušan L., 2008, Contrib. Astron. Obs. Skaln. Pleso, 38, 33
Jiménez-Torres J. J., Pichardo B., Lake G., Throop H., 2011, Mon. Not. R. Astron. Soc., 418, 1272
Kasting J. F., Whitmire D. P., Reynolds R. T., 1993, Icarus, 101, 108
Kirkby J., 2007, Surv. Geophys., 28, 333
Kobayashi H., Ida S., 2001, Icarus, 153, 416
Kopparapu R., et al., 2013, Astrophys. J., 765, 131
Kroupa P., 2001, Mon. Not. R. Astron. Soc., 322, 231
Kunder A., et al., 2012, Astron. J., 143
Lestrade J.-F., Morey E., Lassus A., Phou N., 2011, Astron. Astrophys., 532, A120
Li G., Adams F. C., 2015, Mon. Not. R. Astron. Soc., 448, 344
Lyttleton R. A., Yabushita S., 1965, Mon. Not. R. Astron. Soc., 129, 105
Malmberg D., Davies M. B., Heggie D. C., 2011, Mon. Not. R. Astron. Soc., 411, 859

Martínez-Barbosa C. A., Jílková L., Portegies Zwart S., Brown A. G., 2017, Mon. Not. R. Astron. Soc., 464, 2290

Marzari F., Picogna G., 2013, Astron. Astrophys., 550, A64

Matese J. J., Lissauer J. J., 2002, Icarus, 157, 228

Matese J. J., Whitman P. G., Innanen K. A., Valtonen M. J., 1995, Icarus, 116, 255

Mazeeva O. A., 2004, Sol. Syst. Res., 38, 325

Oort J. H., 1950, Bull. Astron. Institutes Netherlands, 11, 91

Ostriker E. C., 1994, Astrophys. J., 424, 292

Pandey O. P., Negi J. G., 1987, Geophys. J. R. Astron. Soc., 89, 857

Picogna G., Marzari F., 2014, Astron. Astrophys., 564, A28

Portail M., Wegg C., Gerhard O., Martinez-Valpuesta I., 2015, Mon. Not. R. Astron. Soc., 448, 713

Portegies Zwart S. F., Jílková L., 2015, Mon. Not. R. Astron. Soc., 451, 144

Rahvar S., 2017, Mon. Not. R. Astron. Soc., 470, 3095

Rampino M. R., 2015, Mon. Not. R. Astron. Soc., 448, 1816

Rein H., Liu S.-F., 2011, Astron. Astrophys.

Rein H., Spiegel D. S., 2014, Mon. Not. R. Astron. Soc., 446, 1424

Rich R. M., Reitzel D. B., Howard C. D., Zhao H., 2006, Astrophys. J., 688, 1060

Rickman H., Froeschlé C., Froeschlé C., Valsecchi G. B., 2004, Astron. Astrophys., 428, 673

Ruderman M. A., 1974, Science, 184, 1079

Saito R. K., et al., 2011, Astron. Astrophys., 537

Shaviv N. J., 2003, New Astron., 8, 39

Tanaka H. K., 2006, J. Atmos. Solar-Terrestrial Phys., 68, 1396

Vincke K., Breslau A., Pfalzner S., 2015, Astron. Astrophys., 577, A115

Wegg C., Gerhard O., 2013, Mon. Not. R. Astron. Soc., 435, 1874

Wickramasinghe J. T., Napier W. M., 2008, Mon. Not. R. Astron. Soc., 387, 153

Wignall P. B., 2001, Earth Sci. Rev., 53, 1

Zwart S. P., Pelupessy I., van Elteren A., Wijnen T., Lugaro M., 2018, Astron. Astrophys., 616, A85

This paper has been typeset from a TeX/LaTeX file prepared by the author.